Deposition of Latex Colloids at Rough Mineral Surfaces: An Analogue Study Using Nanopatterned Surfaces

ARTICLE *in* LANGMUIR · MARCH 2012

Impact Factor: 4.46 · DOI: 10.1021/la3003146 · Source: PubMed

7 AUTHORS, INCLUDING:

Cornelius Fischer
Universität Bremen
73 PUBLICATIONS **411** CITATIONS
SEE PROFILE

Johannes Lützenkirchen
Karlsruhe Institute of Technology
118 PUBLICATIONS **1,328** CITATIONS
SEE PROFILE

Thorsten Schäfer
Karlsruhe Institute of Technology
165 PUBLICATIONS **1,963** CITATIONS
SEE PROFILE

Frank Heberling
Karlsruhe Institute of Technology
21 PUBLICATIONS **193** CITATIONS
SEE PROFILE

Langmuir

Article

pubs.acs.org/Langmuir

Deposition of Latex Colloids at Rough Mineral Surfaces: An Analogue Study Using Nanopatterned Surfaces

Gopala Krishna Darbha,*[,†,‡] Cornelius Fischer,[†,§] Alex Michler,[†] Johannes Luetzenkirchen,[‡] Thorsten Schäfer,[‡,⊥] Frank Heberling,[‡] and Dieter Schild[‡]

[†]Department of Sedimentology and Environmental Geology, Georg-August-Universität Göttingen, GZG, Goldschmidtstr. 3, D-37077 Göttingen, Germany

[‡]Institute for Nuclear Waste Disposal (INE), Karlsruhe Institute of Technology (KIT), P.O. Box 3640, D-76021 Karlsruhe, Germany

[§]Department of Earth Science, Rice University, 6100 Main Street, Houston, Texas 77005, United States

[⊥]Department of Earth Sciences, Institute of Geological Sciences, Freie Universität Berlin, Berlin, Germany

ABSTRACT: Deposition of latex colloids on a structured silicon surface was investigated. The surface with well-defined roughness and topography pattern served as an analogue for rough mineral surfaces with half-pores in the submicrometer size. The silicon topography consists of a regular pit pattern (pit diameter = 400 nm, pit spacing = 400 nm, pit depth = 100 nm). Effects of hydrodynamics and colloidal interactions in transport and deposition dynamics of a colloidal suspension were investigated in a parallel plate flow chamber. The experiments were conducted at pH ∼ 5.5 under both favorable and unfavorable adsorption conditions using carboxylate functionalized colloids to study the impact of surface topography on particle retention. Vertical scanning interferometry (VSI) was applied for both surface topography characterization and the quantification of colloidal retention over large fields of view. The influence of particle diameter variation (d = 0.3−2 μm) on retention of monodisperse as well as polydisperse suspensions was studied as a function of flow velocity. Despite electrostatically unfavorable conditions, at all flow velocities, an increased retention of colloids was observed at the rough surface compared to a smooth surface without surface pattern. The impact of surface roughness on retention was found to be more significant for smaller colloids (d = 0.3, 0.43 vs. 1, 2 μm). From smooth to rough surfaces, the deposition rate of 0.3 and 0.43 μm colloids increased by a factor of ∼2.7 compared to a factor of 1.2 or 1.8 for 1 and 2 μm colloids, respectively. For a substrate herein, with constant surface topography, the ratio between substrate roughness and radius of colloid, Rq/r_c, determined the deposition efficiency. As Rq/r_c increased, particle−substrate overall DLVO interaction energy decreased. Larger colloids (1 and 2 μm) beyond a critical velocity (7×10^{-5} and 3×10^{-6} m/s) (when drag force exceeds adhesion force) tend to detach from the surface irrespective of the impact of roughness. For polydisperse solutions, an increase in the polydispersity and flow velocity resulted in a reduction of colloid deposition efficiency due to the resulting enhanced double-layer repulsion. Quantification of surface topography variations of two endmembers of natural grain surfaces showed that half-pore depths and roughness of sedimentary quartz grains are mainly in the micrometer range. Grains with diagenetically formed quartz overgrowths, however, show surface roughness mainly in the submicrometer range. Thus, surface topography features applied in the here presented analogue study and resulting variation in particle retention can serve as quantitative analogue for particle reactions in diagenetically altered quartz sands and sandstones. The reported impact of particle polydispersity can have an important application for quantitative prediction of retention of varying types of minerals, such as different clay minerals in the environment under prevailing unfavorable conditions.

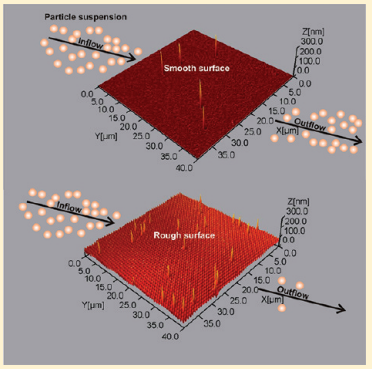

INTRODUCTION

Understanding the colloidal particle deposition mechanism at fluid−solid interfaces is important to address a variety of environmental and industrial processes. Important examples are the protection from particle adsorption in semiconductor manufacturing,[1] the control of colloidal deposition (such as polypeptides) in bioengineering,[2] the transport of pathogenic microorganisms,[3] and heavy metals[4] in the aquatic system as well as the prediction of colloid formation and deposition in nuclear waste repositories.[5,6] Numerous studies have been conducted to investigate the significant factors governing the particle retention mechanisms in the subsurface environments focusing on fluid phase composition,[7,8] the properties of colloids and media,[9] and physical and chemical conditions of the flow.[10−13]

Though there are various hypotheses proposed in the literature to explain the deviation from the traditional classical colloid filtration theory (CFT),[14,15] until now the fate of colloid transport and retention is still poorly understood. As a consequence, the quantitative prediction of particle retention

Received: January 20, 2012
Revised: March 14, 2012
Published: March 26, 2012

in nature (at mineral, rock, and soil surfaces) is still almost impossible. The transport and deposition of colloidal particles in porous media such as sediments or consolidated rocks under unfavorable conditions is of great importance to understand the capture of particles in the environment.[15,16] This is especially true because in most of the cases adsorption of colloids in nature takes place under unfavorable adsorption conditions. The reason for this is that most of the silicate minerals, e.g., quartz, feldspar, and sheet silicates, are negatively charged over a wide range of the pH. The point of zero charge of these minerals is at comparatively low pH.[17−20] The mentioned minerals are ubiquitous in nature and make up significant portions of sedimentary, magmatic, and metamorphic rocks in the earth's crust. Moreover, sheet silicates are a common group of minerals formed due to rock weathering. Because they can be transported over significant distances in the saturated and unsaturated zone, they play a crucial role as colloidal particles in the environment. The above-mentioned common negative charge of many rock-forming minerals, the attachment of clay mineral colloids at rock surfaces will often take place under electrostatically unfavorable conditions.[17−20]

Several studies do suggest that the adsorption of clay mineral particles is a quantitatively very important process in sediments, and as a result, crusts of infiltrated and adsorbed clay minerals are formed.[21] In many natural processes, deposition of colloids on surfaces is explained by chemical and charge heterogeneities of surfaces, impurities, etc.[22] However, under unfavorable conditions, where repulsive forces between mineral surface and particles prevail, an increase of the importance of roughness for deposition of colloids was concluded, and the quantitative impact of surface roughness has to be included into predictive considerations.[23,24]

Though theoretical and experimental investigations suggest an enhanced colloid deposition with increasing surface roughness, data from substrate roughness are not available. Also, the natural fluid−rock interface consists of a wide range of surface topography variances; e.g., iron oxide and clay mineral rims on sedimentary quartz or feldspar grains do alter significantly the initial collector surface roughness.[25,26] The unfavorable retention of colloids in nature is therefore also characterized by a potential alteration of the amount of "*surface roughness*" during ongoing reaction. Recent experimental work conducted at in underground research laboratories (URL)[27,28] and laboratory[29] in the context of colloid mediated radionuclide migration depict the deposition of colloids at rough rock and mineral surface under unfavorable conditions.[27,28] More detailed, batch sorption experiments were performed to study the interaction of gold nanoparticles with rough granite interfaces.[23,30] The experimental comparison of favorable vs unfavorable electrostatic conditions showed non-negligible colloidal retention at the crystalline rock under unfavorable electrostatic conditions influenced by surface roughness. Results of experiments performed by Das and coauthors demonstrated that surface roughness provides a large enough restraining torque in predicting the hydrodynamic detachment of particles.[31] In the experiments carried out for colloid straining and filtration in saturated porous media, the surface roughness of the grains caused an increased colloidal retention due to enhanced collision efficiency by a factor of 2−3.[32,33] Calculations of DLVO interaction energy between a sphere and simulated membrane surfaces predict a significant reduction in the energy barrier with increasing surface roughness.[34,35] Furthermore, experimental results show that the van der Waals (vdW) contact interactions of a polystyrene latex sphere and rough silicon substrate reduced the interaction energy by 90% because of the effective larger separation distance between them.[36]

In light of these observations and calculations, deeper insight into the interaction between particles and rough surfaces is required. The questions how surface roughness variations of the substrate can influence the colloidal deposition, what fundamental processes are related to the removal of fine particles from rough surfaces in a hydrodynamic flow, and what are the preferred sites for particle deposition related to substrate surface roughness or charge variations are still unanswered. More specifically, the interplay between (i) applied hydrodynamics, (ii) the variation of colloid size and polydispersity, and (iii) substrate surface topography variation (roughness) during the complex deposition process requires deep quantitative insight. Most of the theoretical work is based on the interfacial study between positive protrusions and spherical colloids where the particle is several orders of magnitude larger in size compared to the asperity.[37,38] The importance of interaction between a surface with negative asperities (pits/holes/etchpits) was investigated in context to the recent colloid probe technique experiments on a rough membrane composed of peaks and valleys.[39] While results predict that peaks have a decreased magnitude of electrostatic double-layer (EDL) repulsions compared to valleys, the adhesion rate was found to be higher for valleys compared to peaks.[35,37,38] This agrees with recent colloid deposition study on a rough mineral surface (etched calcite) where etch pit walls were the preferred adsorption sites. Moreover, the deposition rate was shown to be a function of etch pit depth and density.[24]

To address potential colloidal adhesion pathways in the environment, in this study a synthetic substrate surface is applied to mimic the natural mineral surfaces and to provide well-defined surface topography (half-pores) for deposition experiments. Here, we investigate and quantify the deposition of polystyrene particles under varying hydrodynamic conditions on an (oxidized) silicon wafer surface with constant surface roughness due to well-defined, regular distribution of holes as a function of size, surface charge, and polydispersity of colloids. A constant surface roughness was applied to study in detail the impact of hydrodynamic parameter variations that are important for deposition at rough surfaces. For our experimental approach we used monodisperse (0.3−2 μm) as well as a polydisperse (bimodal) particle size distribution of polystyrene latex spheres to represent important modes of natural grain-size distribution ranges. We then compare quantitative results about the retention of colloids on smooth and structured surfaces under both favorable and unfavorable conditions. The impact of colloid size and polydispersity on deposition at smooth vs rough oxidized surface employing varying flow rates was studied.

MATERIALS AND METHODS

Colloidal Particles and Silicon Wafer Surface Preparation. Carboxylate polystyrene latex colloids of size 0.3, 0.43, 1, and 2 μm were purchased from Postnova Analytics (Landsberg, Germany). Zeta potentials and photon correlation spectroscopy (PCS) measurements of the colloids were obtained with a ZetaPlus (Zeta Potential Analyzer, Brookhaven Instruments Corp.). The Smoluchowski equation was applied to convert electrophoretic mobility measurements of the colloids to zeta potentials.[40] The zeta potential measurements were performed at pH 5.5 in 10^{-2} M NaCl. The respective zeta potential values for 0.3, 0.43, 1, and 2 μm were −52, −63, −45, and −47 mV.

dx.doi.org/10.1021/la3003146 | *Langmuir* 2012, 28, 6606−6617

The constant average diameters for the polydisperse colloid mixture(s) from the PCS measurements show that suspensions are stable for the duration of the experiments.

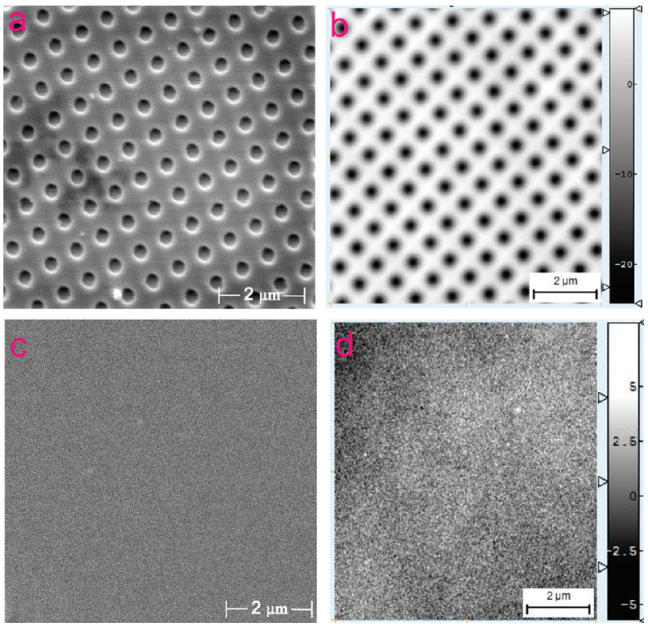

Figure 1. Rough and smooth silicon wafer surface data from SEM and vertical scanning interferometry: (a) rough SEM, (b) rough VSI, (c) smooth SEM, and (d) smooth VSI.

Silicon wafers with (100) orientation were purchased from AMO GmbH, Aachen, Germany. The silicon topography for the rough substrate consists of a regular pit pattern (pit diameter = 400 nm, pit spacing = 400 nm, pit depth = 100 nm), and the smooth substrate was without holes. Wafers were cleaned by consecutive sonication in acetone and isopropanol followed by piranha acid. After thorough rinsing in water, before the wafers were used as substrates for colloid deposition experiments, they were left in air for complete oxidation for 5−7 days. For surface functionalization with APTES (Sigma-Aldrich), the substrates were cleaned with piranha acid and rinsed with water. Subsequently, they were dried under a flow of pure nitrogen. The dry substrates were then immersed in a 10% APTES in methanol solution for 60 min followed by thorough rinsing in methanol and again dried under flow of nitrogen.[41] A thickness of ∼0.9 and ∼0.6 nm for SiO_2 and APTES layers was measured using XPS. Mg Kα (1253.6 eV) X-ray excitation was applied, the angle (electron analyzer−surface normal) 20°, the solid angle of analyzer acceptance ±2°, and analysis area 2 mm diameter. The SiO_2 film thickness was calculated from the elemental Si 2p line intensities assigned to SiO_2 and Si^0 after Shirley background subtraction. These values were in agreement with that reported in the literature.[41,42] Typical dimensions of each silicon sample were 4 mm × 4 mm × 0.68 mm. AFM force volume measurements (Bruker Dimension 3100 atomic force microscope, equipped with a nanoscope IV controller) reveal a uniform surface charge distribution without any heterogeneity (Figure 2).

Experiments were performed at room temperature (22 °C) and at pH ∼ 5.5. The specific conductivity of the water was 0.054 μS/cm. The chemicals (NaCl, APTES) used throughout this study are of research grade and were purchased from Merck and used without any further purification steps.

The zeta potential of both oxidized and APTES functionalized silicon wafer surfaces was determined by a streaming potential analyzer (Anton Paar SurPASS electrokinetic analyzer) with plane-parallel channel cell method at ionic strength of 10^{-2} M NaCl solution. The isoelectric point (IEP) for oxidized silicon surfaces was found to be at pH ∼ 3, and that of APTES functionalized silicon surfaces was found to be at pH ∼ 5.5 (Figure 3).

For each size class the particle concentration was adjusted to 24 × 10^6 particles/mL in 10^{-2} M NaCl solution. In the case of polydisperse colloid mixture solutions, equal particle number concentrations (24 × 10^6 particles/mL) of each size fraction were fixed. All the experiments were conducted in Teflon containers. A blank experiment was conducted to verify no significant loss of colloids within the experimental setup.

Deposition Experiments. The colloidal deposition experiments were conducted in a rectangular parallel-plate channel fluid cell made of Teflon (Figure 4). The inner dimensions of the cell were 60 mm × 10 mm × 3.4 mm. The substrate was oriented parallel to the flow direction. After use, the particle suspension was discarded. For comparison and in order to quantify the influence of half-pores on the substrate surface, the colloid deposition experiments were conducted for both plane and rough substrates.

The time frame of deposition of colloids was fixed to 40 min. The Peclet number and the Reynolds number for the parallel plate flow chamber were calculated based on eqs 1 and 2:[43]

$$Pe = \frac{3Q_{pp}r_c^3}{4wb^3D_\infty} \quad (1)$$

$$Re = \frac{\rho Q_{pp}}{(w + 2b)\upsilon} \quad (2)$$

where Q_{pp} is the flow rate, r_c particle radius, w width of the flow chamber, b half-depth of a parallel plate flow chamber, D_∞ particle diffusion coefficient, ρ fluid density, and υ viscosity.

The volumetric flow rate in cell was adjusted to obtain the required Peclet number. For experiments with individual colloid deposition experiments the implemented Peclet number range of 10^{-4}−1 corresponds to variant flow rate depending on the size of the colloid (from eq 1). In the case of polydisperse colloid suspensions, at a constant flow rate, the Peclet number is the characteristic of each particle size. At the here applied flow rates, the Reynolds numbers are in the range of 0.004−26.

Surface Topography Analysis and Quantification of Colloidal Deposition. The characterization and quantification of surface topography of collector surfaces was carried out with a ZeMapper vertical scanning interferometry (VSI), manufactured by Zemetrics Inc., Tucson, AZ. Vertical resolution of the instrument was <1 nm.[44] Test measurements using a calibration sample showed that objects of a lateral dimension of at least 0.15 μm are detectable on the here applied surface structure at highest magnification (100 × 1.6, field of view: 93 μm × 93 μm, virtual pixel length 45 nm). White light mode was applied for all measurements. Three-dimensional data sets obtained by VSI were used for detailed particle deposition characterization and quantification by Scanning Probe Image Processing (SPIP) software (Image Metrology). For natural quartz surfaces, the approach of converged roughness parameters[45] was applied for the comparison of roughness differences.

Root-mean-square roughness (Rq) was employed to describe the surface roughness of the substrate. Rq is an amplitude parameter and is used to describe the dispersion of the height distribution. It is the sample standard deviation and describes the deviation of measured surface points from the mean or another reference surface, for example, a "zero" (unreacted) plane. For calculation of Rq the surface is considered as a set of N profiles. Each profile has a number of M points.

$$Rq = \sqrt{\frac{1}{MN}\sum_{k=0}^{M-1}\sum_{l=0}^{N-1}[z(x_k, y_l)]^2} \quad (3)$$

For the current approach, as surfaces with defined topography were applied, Rq is the characteristic overall representation factor for size, depth, and distance between pits. The parameter $R10$ is the average height of the five highest local maxima plus the average height of the five lowest local minimums:

dx.doi.org/10.1021/la3003146 | Langmuir 2012, 28, 6606−6617

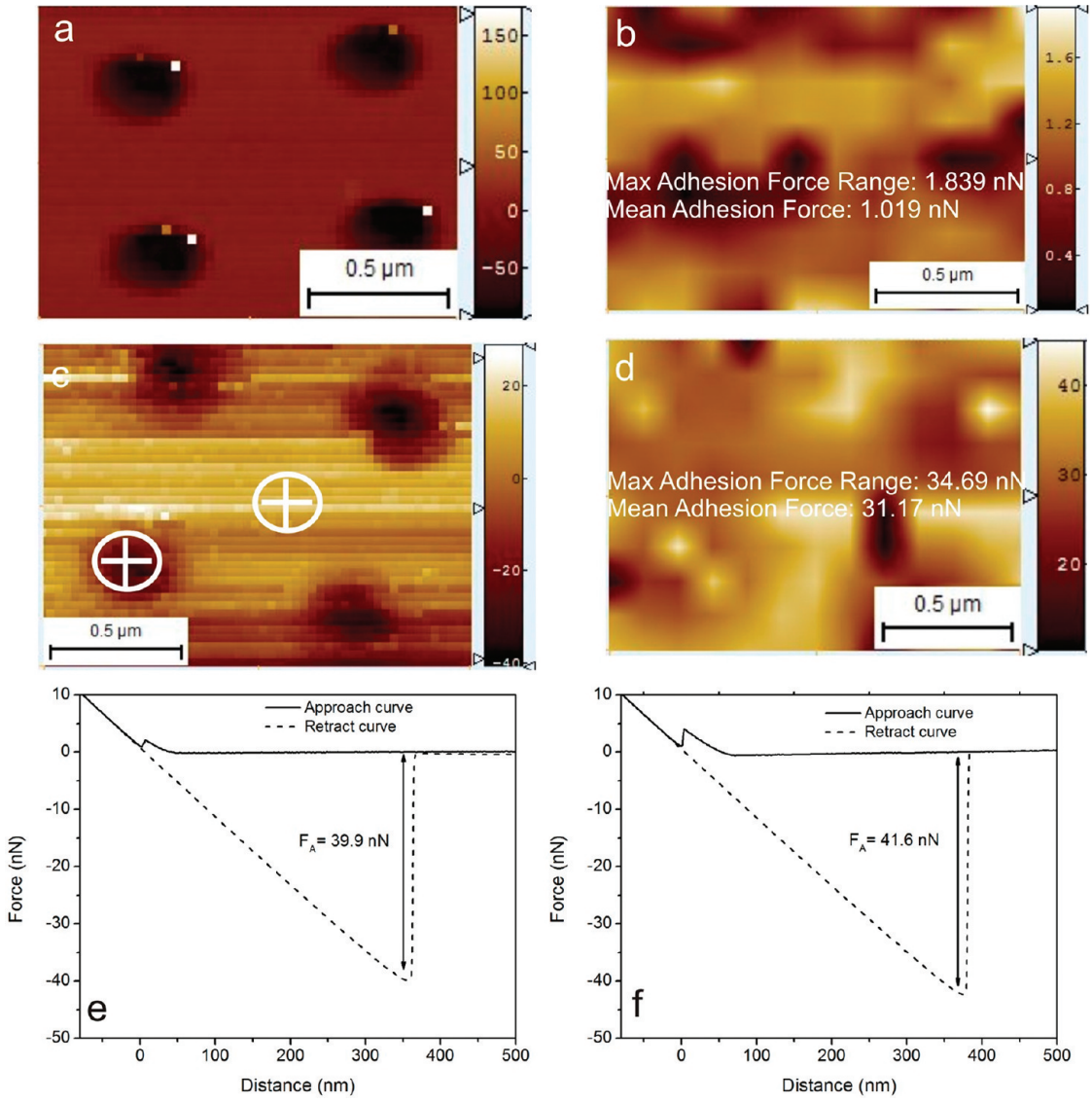

Figure 2. (a) Topography image obtained during force−volume measurements on the silicon wafer using a silica tip. (b) Corresponding maximum adhesion force mapping for silica tip. (c) Topography image obtained during force−volume measurements on the silicon wafer using a 1 μm polystyrene colloid. (d) Corresponding maximum adhesion force mapping for 1 μm colloid, (e, f) Force−distance curves inside a hole and on the flat surface (marked with circle in part c).

$$R10 = \frac{\sum_{i=1}^{5} |z_{pi}| + \sum_{i=1}^{5} |z_{vi}|}{5} \quad (4)$$

The colloid deposition flux, J, and colloid deposition efficiency was determined from eq 5[11]

$$J = \frac{N/A}{TC_0} \quad (5)$$

where N is the number of colloids, A is the scan area, T is time in seconds, and C_0 is initial colloid concentration.

RESULTS AND DISCUSSION

Influence of Surface Roughness on Colloid Deposition. The data of colloid deposition flux for varying colloid diameter at constant flow velocity on silica substrate with holes (rough surface) and smooth surface under favorable (APTES-coated layer) and unfavorable (SiO_2 layer) conditions are presented in Figure 5.

Favorable Conditions (APTES-Coated Surfaces). Regardless of particle diameter, the colloid deposition flux is always higher for an APTES-coated surface (favorable) compared to a silicon oxide surface (unfavorable). For an 0.3 μm colloid it results in a ratio of ~4.8. This is because of the electrostatic attraction between the positively charged silica surface (exposed amino groups) and the high negative surface charge of latex colloids.[46] The resulting high colloid deposition rate is attributed to an increase in range and magnitude of the attractive DLVO interactions. The particle deposition in the absence of energy barrier showed initial decrement with the size, followed by an increase. Moreover, in the absence of an energy barrier, for colloidal particles the gravitational force is not an important factor.[47] The observed minimum deposition flux corresponded to 1 μm colloids with a minor difference for that of 2 μm. The slight increment in J for colloids with d = 2 μm vs d = 1 μm could be attributed to the stronger electrostatic forces of attraction with increasing size of the particle.[47] The 0.3 μm colloids experienced the highest difference in J for smooth

dx.doi.org/10.1021/la3003146 | Langmuir 2012, 28, 6606−6617

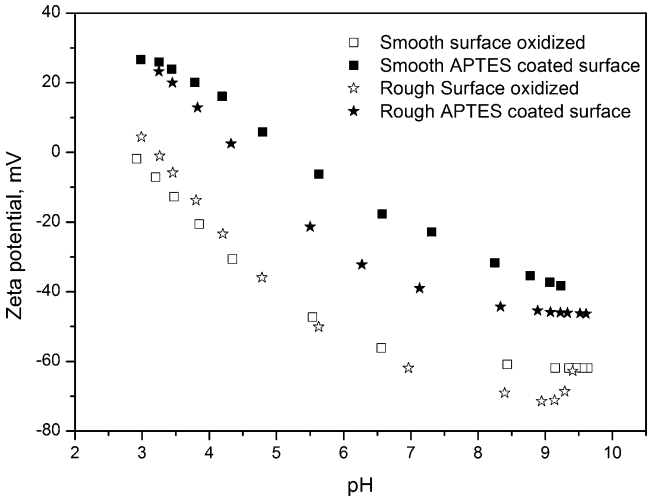

Figure 3. Streaming potential measurements of the smooth (oxidized and APTES coated) and rough (oxidized and APTES coated) silicon wafer samples. The IEP of smooth and rough oxidized silica was ~3. The IEP of smooth and rough APTES coated silica was ~5.5.

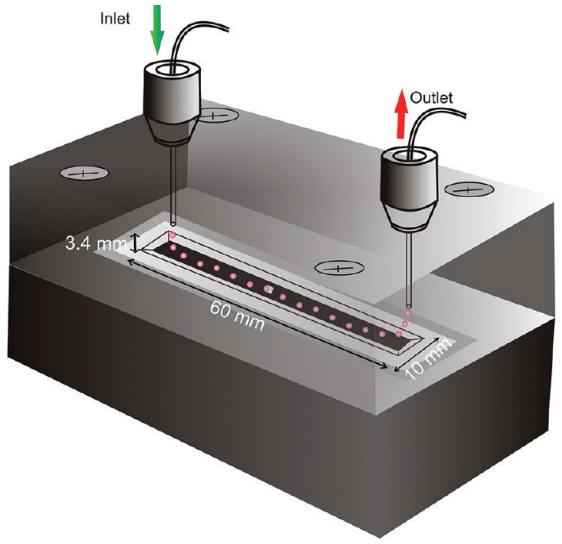

Figure 4. Schematic diagram of the flow cell.

(average Rq = 1.6 ± 0.3 nm) vs rough (average Rq = 18.2 ± 0.4 nm) substrates, and the value decreased with an increase in particle size. Thus, it can be noticed that the effect of surface roughness is more pronounced for smaller colloids compared to larger colloids. The particles beyond 1 μm did not experience any influence of surface roughness.

Unfavorable Conditions. In general, silicon substrates covered by a SiO_2 layer show a decrease of colloid deposition compared to APTES-coated surfaces because of stronger electrical double-layer repulsions. Similar to the previously reported favorable conditions, both effects were again observed: the rough surface shows generally higher deposition rates, and deposition is more effective for smaller particles. A 2.8 and 2.73 times increase in colloidal deposition for a rough vs smooth surface was observed for 0.3 and 0.43 μm colloids. This was the highest observed ratio compared to a factor of 2.1 for 1 μm or 2.4 for 2 μm colloid. As DLVO theory predicts, the height of the energy barrier is proportional to the size of the particles approaching the interfaces. For a fixed DLVO potential of

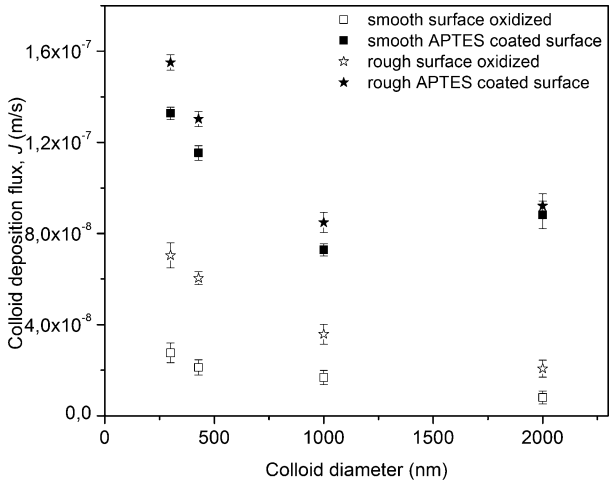

Figure 5. Comparison of colloid deposition flux of carboxylated latex colloids of different sizes at constant fluid velocity (1.3×10^{-5} m/s) for smooth and rough surfaces. The influence of surface roughness on particle retention is smaller for larger colloids and under unfavorable conditions.

particle and surface, the potentials control the magnitude of the double-layer interaction energy and, thus, may have an effect on the particle deposition rates.[47,48] This explains the reason for the decrease of J with increasing colloid size under unfavorable conditions.

Generally, as a particle approaches a rough surface, the repulsive energy barrier height is reduced. This is because of the effectively larger separation distance between a spherical particle and a rough vs smooth surface.[49] Therefore, rough surfaces are more favorable for particle deposition.[35,38] According to previous studies, the influence of roughness is important under unfavorable conditions.[23,46] As reported in the literature, the deposition under repulsive EDL is attributed to colloid attachment with substrate via secondary energy minima, and hence CFT is not applicable.[11] It is evident that electrostatic and acid−base interactions decay more rapidly than vdW interactions, and hence the surface roughness promotes colloidal adhesion irrespective of the chemical properties of substrate material.[34] We interpret therefore the differences in J observed (compared to J for favorable conditions) as a combined effect of charge and roughness. Numerical simulations by Hoek et al. also indicate that for rough surfaces the interaction energy barrier height is primarily determined by the zeta potentials of the surfaces.[34,35] The efficiency of roughness-governed particle retention seems to be at maximum in the presence of an energy barrier. Therefore, we performed the below discussed systematic experimental approach by varying particle size and fluid flow velocity to understand particle retention at rough vs smooth surface in the presence of energy barrier.

Impact of Particle Size Variation and Fluid Flow Velocity Variation on Particle Retention at Given Rough vs Smooth Surface Topography. The systematic study of colloidal particle deposition under varying flow rates at smooth vs rough SiO_2 substrates (Figure 6) showed independent deposition behavior with respect to substrate roughness. In the presence of an energy barrier, at all fluid velocities, both smooth and rough surfaces exhibited a variable colloid deposition behavior with maximum deposition for 0.3 μm colloids. Moreover, independently of the applied fluid velocity the

dx.doi.org/10.1021/la3003146 | Langmuir 2012, 28, 6606−6617

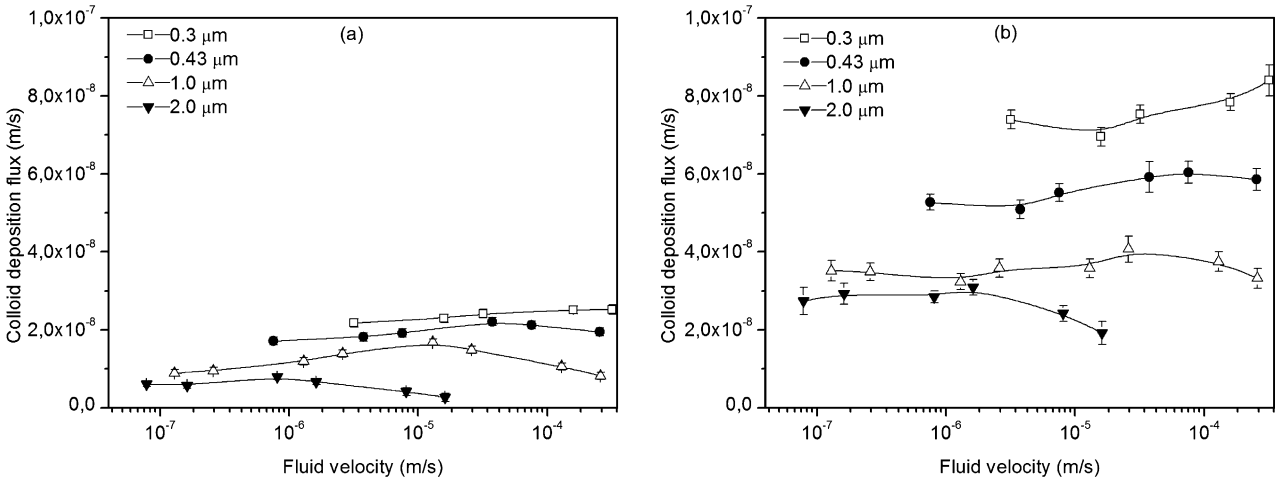

Figure 6. Colloid deposition flux at smooth (a) and rough (b) oxidized silicon wafer substrates. For smooth surfaces, beyond a critical velocity (for 1 μm it is 10^{-5} m/s) the rate of colloidal deposition decreased with an increase in colloid size and fluid velocity, while under applied hydrodynamic torque at high flow velocities roughness of the substrate retains colloids onto surface (for 1 μm it is 5×10^{-5} m/s).

rates of deposition fluxes were higher for rough vs smooths. From smooth to rough the deposition rate for smaller colloids (0.3 and 0.43 μm) increased by a factor of ~2.66 compared to bigger colloids (1 and 2 μm), by a factor of 1.2–2. This shows the dependency of colloid deposition on the ratio of the size of the colloid to the roughness value. As the ratio increases, the effective surface contact area with the substrate increases; therefore, less effect of roughness is seen by the particle.

For colloids of all sizes, both kinds of substrates exhibit increased colloid deposition fluxes with initial increment in the fluid velocity. For a smooth surface, beyond a critical velocity based on the size of the colloid, the detachment starts. The tendency to release or transport the larger colloids is initiated at lower velocities compared to the smaller colloid fraction. The 0.3 and 0.43 μm colloids are stable on surface even at high fluid velocities ($<5 \times 10^{-5}$ m/s) while 1 and 2 μm colloids can sustain up to 10^{-5} and 10^{-6} m/s. This shows that the colloids deposited in the secondary minima are subject to removal from the surface under the influence of hydrodynamic force.[10−12] The electrostatic and vdW interactions decay with colloid−surface separation distance at distinct rates, at small separation distances (primary minimum, ~0.4 nm) vdW attraction may greatly dominate, at intermediate distances where particles tend to deposit, electrostatic forces play a role, and at very large distances (secondary minimum, ~5−10 nm) vdW attraction may slightly dominate. Hence, colloids that are attached in the secondary minima are weakly associated with the solid phase. On the other hand, in the case of rough substrates, under the implemented velocities, no influence of hydrodynamic torque on 0.3 and 0.43 μm was observed. Pertaining to greater restraining torque these colloids were retained even at $>10^{-4}$ m/s fluid velocities. The larger colloid fraction, 1 and 2 μm colloids, detached from the surface beyond 10^{-4} and 5×10^{-6} m/s irrespective of the substrate roughness. This shows less pronounced tendencies for surface roughness. Because of the maintained balance between adhesion force over applied torque, it is worth noticing that these velocities are higher at smooth surfaces. Our results are supported by the recent calculations from Shen et al.,[50] which predicted that the attachment efficiency of a colloid does not change until it reaches a critical velocity which is a function of ionic strength, surface properties of colloids, and substrate. Also, a colloid with smaller diameter attains critical velocity at higher flow conditions compared to a colloid with larger diameter.

Particle Retention Mechanisms. According to fundamental studies reported in the literature,[15] when a particle interacts with the substrate, different mechanisms may play a role either for attachment or detachment, such as rolling, dragging, and lifting (Figure 7). As reported from the literature, rolling plays

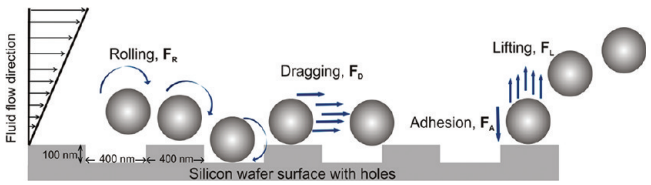

Figure 7. Schematic profile diagram to visualize the common forces at a fluid−solid body interface. As an example, a particle with $d = 0.3$ μm is shown at the structured surface applied for the study reported here.

an important role from the surface under laminar flow conditions. Rolling can be initiated on any particle independent of its size even at the smallest flow rates (i.e., at lowest Reynolds numbers) adopted in the current system.[51] In order for a particle to be removed from the surface, the hydrodynamic torque applied on the particle must exceed that of the adhesion torque.[13] Burdick et al. reported that the lever arm that act on applied torque decreased with increasing size of surface roughness. Unlike a smooth surface, a rough surface can change the point around which the rolling occurs; hence, for a rough surface a larger applied torque is required to remove a particle from the surface.[52]

The hydrodynamic and adhesive forces will have a big impact on that section of the collector surface where retention occurs, and colloids which collide with a collector may roll along the surface until they come to a region that is chemically and hydrodynamically favorable for deposition.[13,15] In the current case, as similar chemical conditions were maintained, rolling is initiated even at low flow velocities. Retention of 0.3 μm particles that can be imbedded into holes is preferable pertaining to higher straining compared to any larger colloid sizes. With increasing colloid size the restraining torque acting

dx.doi.org/10.1021/la3003146 | Langmuir 2012, 28, 6606−6617

on the particles decreases. Simultaneously, the fluid drag force increases which results in lower colloid retention.

The physical forces acting on the particles are dependent on the flow conditions near the particle−substrate interface. The drag force (F_D) effectively acts on the attached particles at a height of $1.4r_c$ (eq 6).[15] An increase in particle size will result in an increased applied torque with vertical velocity gradient on the surface of substrate and may lead to an excessive fluid drag. The larger contact area of the colloid with increasing diameter disables the effect of surface roughness. This means that the impact of surface roughness on colloidal retention is caused by the effective contact area at the interface. Under unfavorable conditions, the particles are deposited in the secondary minimum, and the depth of secondary minima increases with particle size due to van der Waals forces. Simultaneous excess fluid drag (T_{app}) may lead to particle removal from the surface.

$$T_{app} = 1.4r_cF_D \tag{6}$$

where the drag force $F_D = 10.205\pi\mu(\partial V/\partial r)r_c^2$

$$T_{adh} = F_Al_x \tag{7}$$

where r_c is the radius of colloid, F_D the drag force, and F_A the force of adhesion acting on a lever arm l_x (calculated according to ref 12). Here l_x is the radius of the colloid−surface contact area which is calculated according to the Johnson, Kendall, and Robers theory. At secondary minimum, as there is no direct contact between colloid and surface, the value of l_x is given as

$$l_x = \left(\frac{F_Ar_c}{4K}\right)^{1/3} \tag{8}$$

Here K is the composite Young's modulus. $K = 1.332 \times 10^8$ N m^{-2} is based on the force−volume data collected from AFM for polystyrene colloid−silicon wafer collector in 10^{-2} M NaCl solution. This is 1 order of magnitude lower than in the system where polystyrene colloids−glass bead collectors were considered.[53]

Considering the DLVO interaction energy profile between a colloid and a plate, Gregory's superposition approximations was employed to calculate the adhesive force (F_A) that acts on attached colloids.[54] The value of F_A was estimated as Φ_{min}/h, where Φ_{min} is the absolute value of the secondary minimum interaction energy and h is the separation distance between the colloid and the substrate. The calculation from the DLVO interaction energy profile resulted in Φ_{min} of −0.54, −0.72, −1.89, and −3.73 kT for the 0.3, 0.43, 1, and 2 μm colloids, respectively. The obtained value was used to estimate the applied and adhesion (resisting) torque acting on colloids in the secondary minimum using eqs 6 and 7. It can be interpreted from Figure 8 that with an increment in fluid velocity the ratio T_{app}/T_{adh} increases at a higher rate with particle size. As the substrate employed here has constant Rq, with an increase in size of the colloid the ratio Rq/r_c determines the colloid deposition efficiency. For smaller colloids (0.3 and 0.43 μm), the ratio is higher due to an effective contact area with the substrate compared to the larger particles (1 and 2 μm). It is worth noticing that, for all particles, though at lower velocities (10^{-6}−10^{-7} m/s) higher ratios of T_{app}/T_{adh} (5 to 99) can be observed no impact on particle deposition efficiency was observed (Figure 6).

Table 1 represents the comparison between calculated and observed fluid velocities around which the particle detachment is expected. A minimum ratio T_{app}/T_{adh} of >15 900 is needed for a 0.3 μm particle to be removed from the rough surface which is the highest observed value for this system. The impact of surface roughness can be directly seen with increase of T_{app}/T_{adh} (smooth vs rough). In perspective of flow in groundwater systems, it can be concluded that for a colloid size fraction of ≤2 μm, where flow velocities are ≤0.26 m/d, colloid filtration is the dominant mechanism.

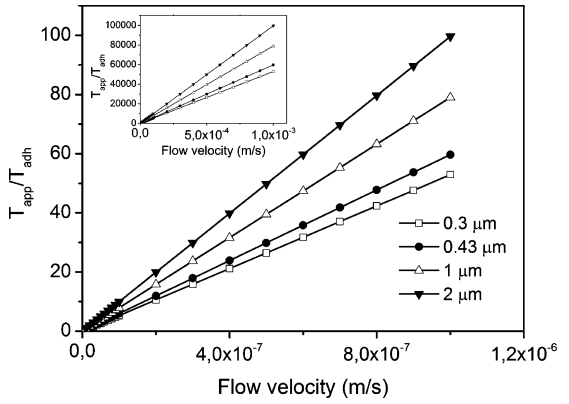

Figure 8. Ratio of T_{app}/T_{adh} at a smooth surface under varying flow rates for all colloid sizes applied in this study. The high probability of particle removal can be predicted when $T_{app} \gg T_{adh}$.

Table 1. Observed Detachment Velocities for All Size Colloids for Smooth vs Rough Substrates[a]

diam of colloid [μm]	approx detachment flow velocity for rough surface [m/s]	T_{app}/T_{adh} (rough)	approx detachment flow velocity for smooth surface [m/s]	T_{app}/T_{adh} (smooth)
0.3	$>3 \times 10^{-4}$ (or ∼26 m/d)	15900	$>10^{-4}$	5290
0.43	$>10^{-4}$ (or ∼8.6 m/d)	5970	$>2 \times 10^{-5}$	1190
1	$>7 \times 10^{-5}$ (or ∼6 m/d)	5530	$>10^{-5}$	790
2	$>3 \times 10^{-6}$ (or ∼0.26 m/d)	299	$>10^{-6}$	99.6

[a]At these velocities, the respective ratio T_{app}/T_{adh} is provided.

Effect of Polydispersity. The results based on deposition experiments with polydisperse colloid suspensions illustrate that an increase in polydispersity leads to a decrease in the deposition efficiency (Figure 9). Roughness showed a prominent affect (J_{smooth}/J_{rough}) when the surface is oxidized and at lower polydispersity ratio 0.3−0.43 μm compared to the larger particle size fraction 0.43−2 μm. Because of interparticle hydrodynamic interactions (hydrodynamic blocking effect),[55,56] when a particle approaches an already adsorbed particle, it will be directed away from the shortest path due to EDL repulsions (Figure 10). The hydrodynamic blocking was found significant (i) when the surface is rough- and APTES coated and (ii) for those flow velocities where any of the particles in the suspension approaches $Pe > 1$. The hindered area is a narrow zone having a width of the order of the particle size.[41] Hence, the electrohydrodynamic blocking increases with an increase in particle size. An increase in velocity also showed a profound influence on polydisperse colloid deposition behavior. The colloid deposition rate decreased with an increase in fluid flow velocity. When a particle is deposited, a hydrodynamic shadow region is created (shadow length). The exclusion zone around the particle is a characteristic of particle size and fluid velocity. At a constant velocity for polydisperse solution, the smaller

dx.doi.org/10.1021/la3003146 | Langmuir 2012, 28, 6606−6617

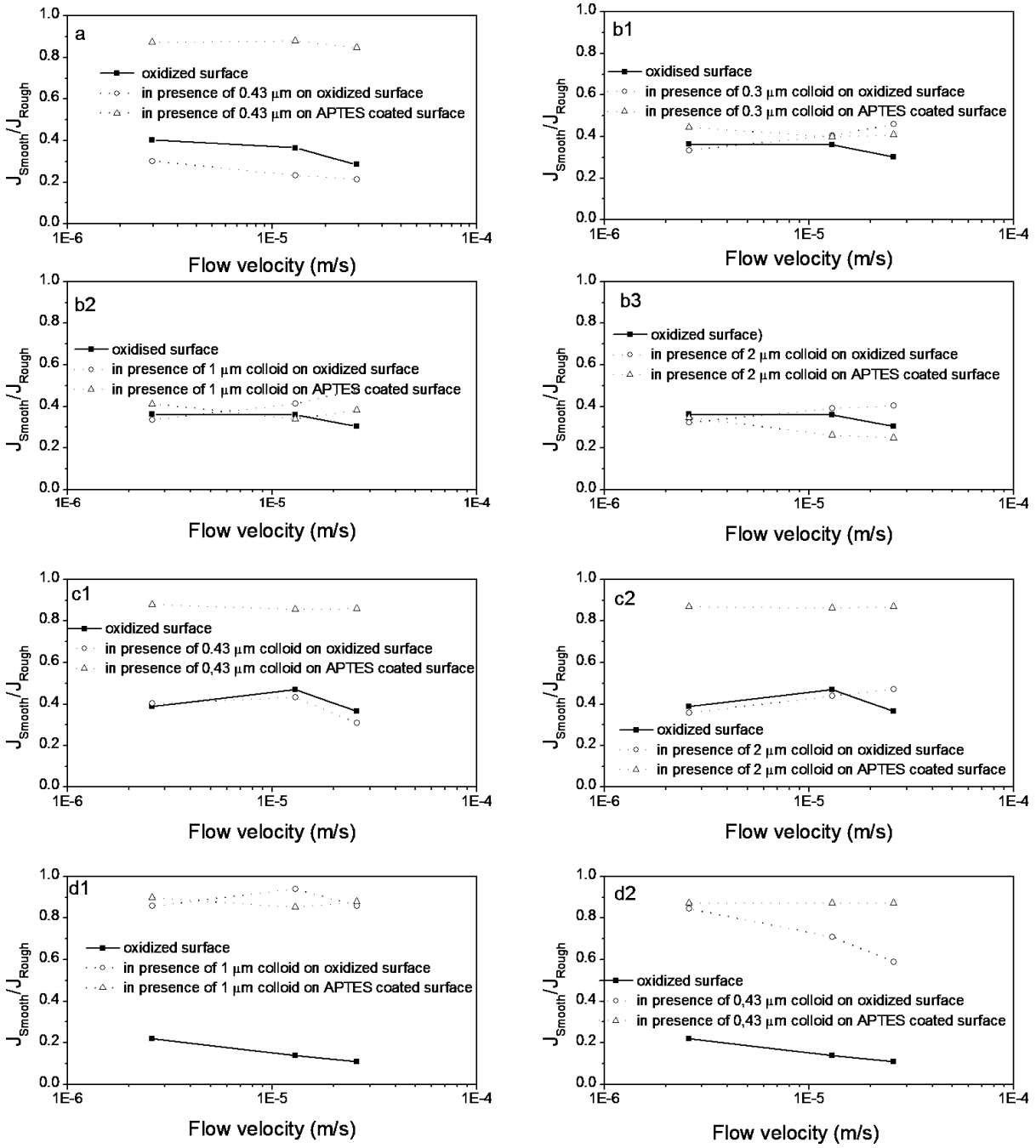

Figure 9. Colloid deposition efficiency for different carboxylated colloid size mixtures of equal particle number concentration at three flow velocities: 2.6×10^{-6}, 1.3×10^{-5}, and 2.6×10^{-5} m/s. (a) Deposition of 0.3 μm colloid; (b1, b2, b3) deposition of 0.43 μm colloid; (c1, c2) deposition of 1 μm colloid; (d1, d2) deposition of 2 μm colloid.

particles experience a high Peclet number compared to larger ones. Smaller particles (<1 μm) and lower fluid velocities result in more efficient diffusive transport and, hence, a smaller shadow region.[57] Though a detailed and thorough investigation was not presented, similar to Loenhout et al.,[41] we can conclude that the blocked area around particles is in the size range of a few orders of the diameter of the particle (Figure 10).

Outlook: Application of Results from Analogue Material (Silicon Wafer) to Natural Material in the Environment. For comparison to the previously discussed regular and artificial surfaces, we discuss now the extent and range of surface topography and roughness parameter variation of natural material that is important for filtration of natural colloids in riverbeds and water-saturated sediments. Specifically, variation in efficiency of colloidal retention at grain surfaces is able to modify and govern subsequent precipitation processes in sand pores.[58] We show two end members of common sedimentary grain surface topographies, i.e., the surface of unconsolidated quartz grains as well as diagenetically formed quartz overgrowth surfaces (Figure 11).

Surface roughness parameters are shown as a function of the observation length (Figure 12). This enables to detect the

dx.doi.org/10.1021/la3003146 | Langmuir 2012, 28, 6606−6617

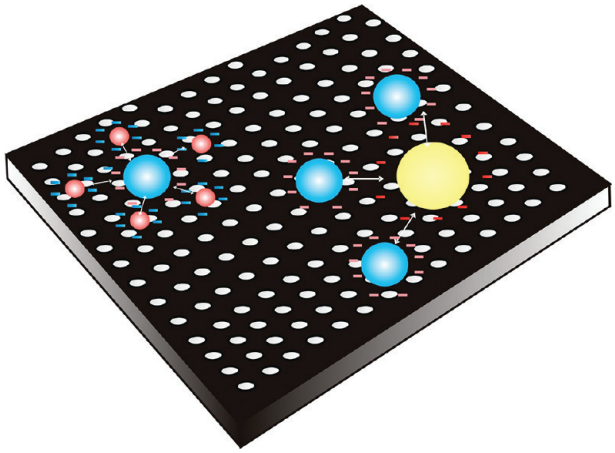

Figure 10. Schematic diagram to explain the increase in particle deposition hindrance with increase in the polydispersity ratio due to electrostatic double-layer repulsions between particles.

extent of roughness parameter variation. This approach is also known as the analysis of converged roughness parameters.[45]

The parameter ten-point height ($R10$) provides information about the amplitude of grain surface topography. For section lengths between 3 and 80 μm for both surface types a variation of almost 2 orders of magnitude of surface height variation has been found. The relief of the sedimentary grain surface is higher than those of the overgrowth, i.e., at micrometer vs submicrometer scale for section length >10 μm. This difference in height variation could also be an important input parameter in terms of filter theory model calculations. In other words: the formation of diagenetically formed grain overgrowths will decrease the asperity of sedimentary grains within at least 1 order of magnitude. This will also affect the efficiency of interception according to filter theory.

Root-mean-square roughness Rq shows a similar trend as discussed for $R10$: According to statistical sensitivity of Rq, the standard deviation of surface topography variation of the two grain surface types differ by about 1 order of magnitude. Accordingly, the overwhelming part of grain surfaces consist of surface steps with heights of several hundreds of nanometers (overgrowth) or around 1 μm (unconsolidated grains). This is the case for the major portion of the here investigated grain surfaces because of the relatively small Rq variation. We therefore conclude that experimental setups using submicrometer surface steps (this study) are able to mimic diagenetically modified, cemented sand grain surfaces. The quantitative result of this study can therefore serve as a direct analogue for predictions. For unconsolidated sediments (no overgrowths) we suggest a sample design with step heights in the 1−10 μm scale for future experiments.

The surface factor F quantifies the total surface area of the grains. F values close to 1 are due to smooth surfaces. Sedimentary grains with diagentically formed overgrowths do have small height variations and show only minor variations in total surface area. Unconsolidated grains, however, show a bigger amount and variation in total surface area. The here reported variation is an important data set for surface area normalization, e.g., for calculations in terms of adsorption density.

SUMMARY

1 A rough topography with surface structures in the submicrometer scale has a significant effect on colloidal deposition under unfavorable conditions rather when surfaces are oppositely charged. Under unfavorable conditions, the deposition efficiency at rough surfaces is increased at least by a factor of 2.7 in case of 0.3 and 0.43 μm and 1.2 and 1.8 for 1 and 2 μm particles compared to smooth surfaces of the same surface charge.

2 The impact of roughness on retention is especially important for small particles. This may explain differences in retention efficiency of mineral colloids in the environment as a function of particle size.

3 Rolling is the fundamental transport mechanism at surfaces to trap preferentially smaller colloids. This results in a high deposition flux over a broad range of fluid velocities.

4 For both smooth and rough collector surfaces the deposition flux increases with fluid velocity. Beyond a

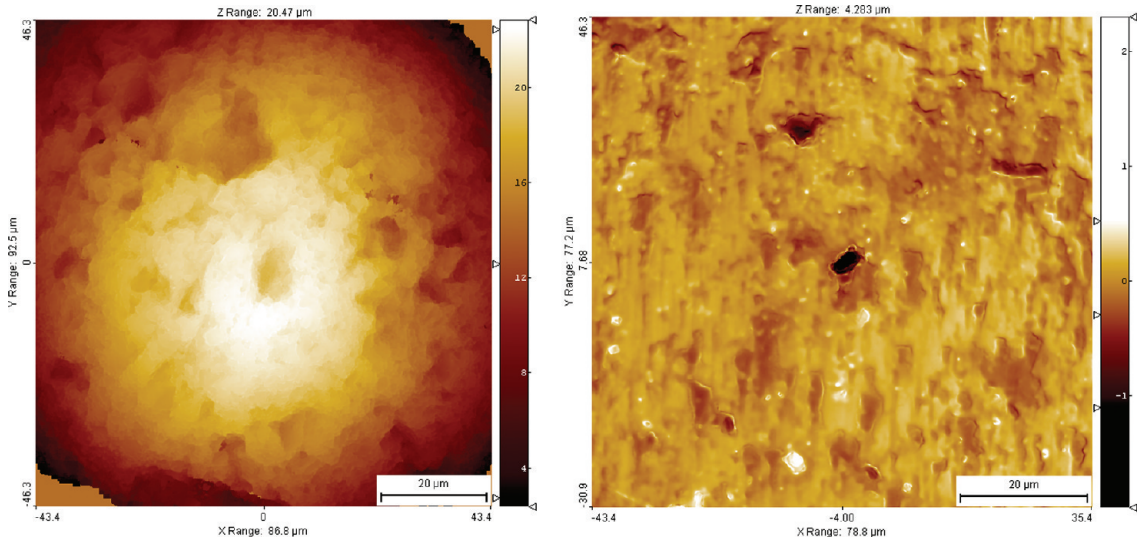

Figure 11. Left side: curved rough surface of a quartz grain without cementation in an unconsolidated sediment. Scale bar: 20 μm, height range: 20.5 μm. Right side: flat surface of a quartz overgrowth. Scale bar: 20 μm, height range: 4.3 μm. Both images were rendered from VSI data sets.

dx.doi.org/10.1021/la3003146 | *Langmuir* 2012, 28, 6606−6617

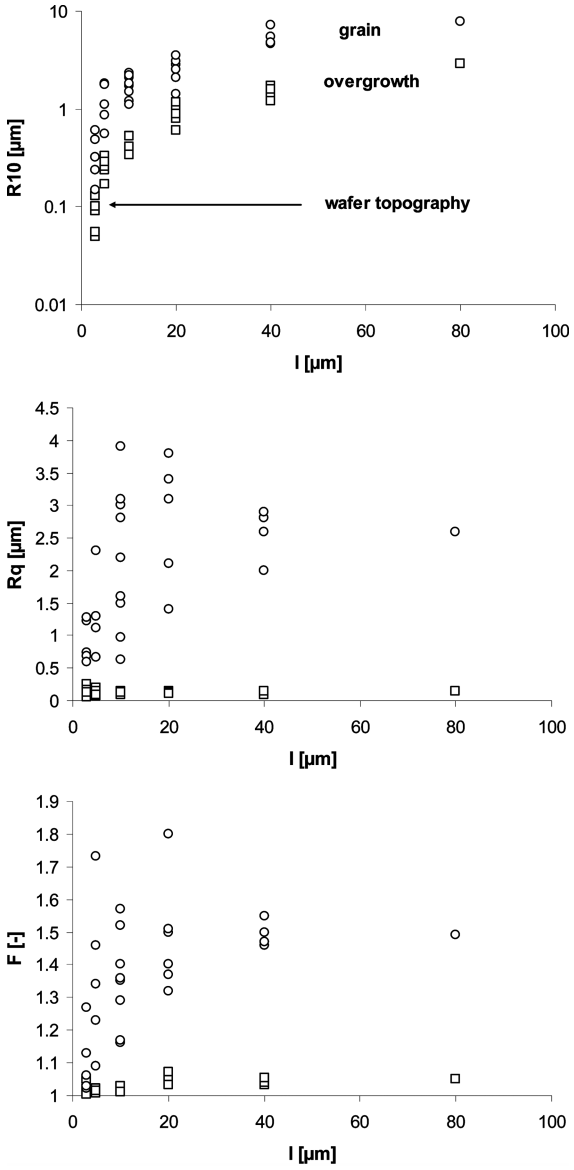

Figure 12. Comparison of surface roughness parameters of uncemented sand grain surfaces (circles) as well as of diagenetically formed quartz overgrowth (squares). The parameters ten-point height ($R10$), root-mean-square roughness (Rq), and surface factor (F) are presented. Parameters are shown as a function of field-of-view length to show the wavelength of parameter variation. For comparison, $R10$ of wafer surface topography is shown, representing the depth of surface pits.

critical velocity, however, the particles detach from surface. Because of higher restraining torque acting at rough collector surfaces, this critical velocity is higher at rough surfaces.

5 The increase in polydispersity results in lower deposition efficiency. The electrostatichydrodynamic blocking (shadow effect) is more efficient at higher polydispersity as well as when the Peclet number is close to 1.

6 The here reported increased particle retention at rough vs smooth surfaces is important for several applications. Minerals in the environment (e.g., sediment grains) with surface topography variations will act as collector surfaces for mineral colloid deposition under electrostatically unfavorable conditions. Important applications are contaminant management as well as early diagenetic reactions in aquifers. Fluid velocity variations in the environment can provoke colloid mobilization from the adsorbent surface. Size variations of natural colloids, e.g., several types of clay minerals or iron oxides, will lead to variations in retention efficiency at mineral and rock–fluid interfaces.

AUTHOR INFORMATION

Corresponding Author

*E-mail: gopala.darbha@kit.edu.

Notes

The authors declare no competing financial interest.

ACKNOWLEDGMENTS

This is publication # GEOTECH-1331 of the GEOTECHNOLOGIEN R&D program funded by the German Ministry of Education and Research (BMBF) and German Research Foundation (DFG). This study was supported by a GEOTECHNOLOGIEN grant to C.F., grant #03G0719A. Financial support by the Federal Ministry of Economics and Technology (BMWi) under the joint research project "KOLLORADO 2" is gratefully acknowledged.

REFERENCES

(1) Heroux, J. B.; Boughaba, S.; Ressejac, I.; Meunier, M. CO_2 laser-assisted removal of submicron particles from solid surfaces. *J. Appl. Phys.* **1996**, *79* (6), 2857–2862.

(2) Zheng, H. P.; Berg, M. C.; Rubner, M. F.; Hammond, P. T. Controlling cell attachment selectively onto biological polymer-colloid templates using polymer-on-polymer stamping. *Langmuir* **2004**, *20* (17), 7215–7222.

(3) Bales, R. C.; Hinkle, S. R.; Kroeger, T. W.; Stocking, K.; Gerba, C. P. Bacteriophage Adsorption during Transport through Porous-Media - Chemical Perturbations and Reversibility. *Environ. Sci. Technol.* **1991**, *25* (12), 2088–2095.

(4) Baumann, T.; Fruhstorfer, P.; Klein, T.; Niessner, R. Colloid and heavy metal transport at landfill sites in direct contact with groundwater. *Water Res.* **2006**, *40* (14), 2776–2786.

(5) Schäfer, T.; Geckeis, H.; Bouby, M.; Fanghänel, T. U, Th, Eu and colloid mobility in a granite fracture under near-natural flow conditions. *Radiochim. Acta* **2004**, *92* (9–11), 731–737.

(6) Schäfer, T.; Seher, H.; Hauser, W.; Walther, C.; Degueldre, C.; Yamada, M.; Suzuki, M.; Missana, T.; Alonso, U.; Trick, T.; Blechschmidt, I. The Colloid Formation and Migration (CFM) project at the Grimsel Test Site (Switzerland): Results from the homologue tests. *Geochim. Cosmochim. Acta* **2009**, *73* (13), A1168–A1168.

(7) Prescott, S. W.; Fellows, C. M.; Considine, R. F.; Drummond, C. J.; Gilbert, R. G. The interactions of amphiphilic latexes with surfaces: the effect of surface modifications and ionic strength. *Polymer* **2002**, *43* (11), 3191–3198.

(8) Schaldach, C. M.; Bourcier, W. L.; Shaw, H. F.; Viani, B. E.; Wilson, W. D. The influence of ionic strength on the interaction of viruses with charged surfaces under environmental conditions. *J. Colloid Interface Sci.* **2006**, *294* (1), 1–10.

(9) Zhuang, J.; Qi, J.; Jin, Y. Retention and transport of amphiphilic colloids under unsaturated flow conditions: Effect of particle size and surface property. *Environ. Sci. Technol.* **2005**, *39* (20), 7853–7859.

(10) Johnson, W. P.; Li, X. Q.; Yal, G. Colloid retention in porous media: Mechanistic confirmation of wedging and retention in zones of flow stagnation. *Environ. Sci. Technol.* **2007**, *41* (4), 1279–1287.

(11) Tong, M. P.; Johnson, W. P. Excess colloid retention in porous media as a function of colloid size, fluid velocity, and grain angularity. *Environ. Sci. Technol.* **2006**, *40* (24), 7725–7731.

(12) Johnson, W. P.; Tong, M. P. Observed and simulated fluid drag effects on colloid deposition in the presence of an energy barrier in an impinging jet system. *Environ. Sci. Technol.* **2006**, *40* (16), 5015−5021.
(13) Torkzaban, S.; Bradford, S. A.; Walker, S. L. Resolving the coupled effects of hydrodynamics and DLVO forces on colloid attachment in porous media. *Langmuir* **2007**, *23* (19), 9652−9660.
(14) Bradford, S. A.; Simunek, J.; Bettahar, M.; Van Genuchten, M. T.; Yates, S. R. Modeling colloid attachment, straining, and exclusion in saturated porous media. *Environ. Sci. Technol.* **2003**, *37* (10), 2242−2250.
(15) Bradford, S. A.; Torkzaban, S. Colloid transport and retention in unsaturated porous media: A review of interface-, collector-, and pore-scale processes and models. *Vadose Zone J.* **2008**, *7* (2), 667−681.
(16) Chang, Y. I.; Chan, H. C. Correlation equation for predicting filter coefficient under unfavorable deposition conditions. *AIChE J.* **2008**, *54* (5), 1235−1253.
(17) Kosmulski, M. The pH-dependent surface charging and the points of zero charge. *J. Colloid Interface Sci.* **2002**, *253* (1), 77−87.
(18) Kosmulski, M. pH-dependent surface charging and points of zero charge - II. Update. *J. Colloid Interface Sci.* **2004**, *275* (1), 214−224.
(19) Kosmulski, M. pH-dependent surface charging and points of zero charge III. Update. *J. Colloid Interface Sci.* **2006**, *298* (2), 730−741.
(20) Kosmulski, M. pH-dependent surface charging and points of zero charge. IV. Update and new approach. *J. Colloid Interface Sci.* **2009**, *337* (2), 439−448.
(21) Matlack, K. S.; Houseknecht, D. W.; Applin, K. R. Emplacement of Clay into Sand by Infiltration. *J. Sediment. Petrol.* **1989**, *59* (1), 77−87.
(22) Filby, A.; Plaschke, M.; Geckeis, H.; Fanghänel, T. Interaction of latex colloids with mineral surfaces and Grimsel granodiorite. *J. Contam. Hydrol.* **2008**, *102* (3−4), 273−284.
(23) Alonso, U.; Missana, T.; Patelli, A.; Ceccato, D.; Albarran, N.; Garcia-Gutierrez, M.; Lopez-Torrubia, T.; Rigato, V. Quantification of Au nanoparticles retention on a heterogeneous rock surface. *Colloids Surf., A* **2009**, *347* (1−3), 230−238.
(24) Darbha, G. K.; Schäfer, T.; Heberling, F.; Luttge, A.; Fischer, C. Retention of Latex Colloids on Calcite as a Function of Surface Roughness and Topography. *Langmuir* **2010**, *26* (7), 4743−4752.
(25) Fischer, C.; Karius, V.; Lüttge, A. Correlation between submicron surface roughness of iron oxide encrustations and trace element concentrations. *Sci. Total Environ.* **2009**, *407*, 4703−4710.
(26) Fischer, C.; Karius, V.; Weidler, P. G.; Luttge, A. Relationship between micrometer to submicrometer surface roughness and topography variations of natural iron oxides and trace element concentrations. *Langmuir* **2008**, *24* (7), 3250−3266.
(27) Mori, A.; Alexander, W. R.; Geckeis, H.; Hauser, W.; Schäfer, T.; Eikenberg, J.; Fierz, T.; Degueldre, C.; Missana, T. The colloid and radionuclide retardation experiment at the Grimsel Test Site: influence of bentonite colloids on radionuclide migration in a fractured rock. *Colloids Surf., A* **2003**, *217* (1−3), 33−47.
(28) Geckeis, H.; Schäfer, T.; Hauser, W.; Rabung, T.; Missana, T.; Degueldre, C.; Mori, A.; Eikenberg, J.; Fierz, T.; Alexander, W. R. Results of the colloid and radionuclide retention experiment (CRR) at the Grimsel Test Site (GTS), Switzerland - impact of reaction kinetics and speciation on radionuclide migration. *Radiochim. Acta* **2004**, *92* (9−11), 765−774.
(29) Delos, A.; Walther, C.; Schäfer, T.; Büchner, S. Size dispersion and colloid mediated radionuclide transport in a synthetic porous media. *J. Colloid Interface Sci.* **2008**, *324* (1−2), 212−215.
(30) Alonso, U.; Missana, T.; Patelli, A.; Rigato, V.; Ravagnan, J. Colloid diffusion in crystalline rock: An experimental methodology to measure diffusion coefficients and evaluate colloid size dependence. *Earth Planet. Sci. Lett.* **2007**, *259* (3−4), 372−383.
(31) Das, S. K.; Schechter, R. S.; Sharma, M. M. The Role of Surface-Roughness and Contact Deformation on the Hydrodynamic Detachment of Particles from Surfaces. *J. Colloid Interface Sci.* **1994**, *164* (1), 63−77.
(32) Auset, M.; Keller, A. A. Pore-scale visualization of colloid straining and filtration in saturated porous media using micromodels. *Water Resour. Res.* **2006**, *42* (12), W12S02, doi:10.1029/2005WR004639.
(33) Shellenberger, K.; Logan, B. E. Effect of molecular scale roughness of glass beads on colloidal and bacterial deposition. *Environ. Sci. Technol.* **2002**, *36* (2), 184−189.
(34) Hoek, E. M. V.; Agarwal, G. K. Extended DLVO interactions between spherical particles and rough surfaces. *J. Colloid Interface Sci.* **2006**, *298* (1), 50−58.
(35) Hoek, E. M. V.; Bhattacharjee, S.; Elimelech, M. Effect of membrane surface roughness on colloid-membrane DLVO interactions. *Langmuir* **2003**, *19* (11), 4836−4847.
(36) Cooper, K.; Gupta, A.; Beaudoin, S. Substrate morphology and particle adhesion in reacting systems. *J. Colloid Interface Sci.* **2000**, *228* (2), 213−219.
(37) Martines, E.; Csaderova, L.; Morgan, H.; Curtis, A. S. G.; Riehle, M. O. DLVO interaction energy between a sphere and a nanopatterned plate. *Colloids Surf., A* **2008**, *318* (1−3), 45−52.
(38) Bhattacharjee, S.; Ko, C. H.; Elimelech, M. DLVO interaction between rough surfaces. *Langmuir* **1998**, *14* (12), 3365−3375.
(39) Bowen, W. R.; Doneva, T. A. Atomic force microscopy studies of membranes: Effect of surface roughness on double-layer interactions and particle adhesion. *J. Colloid Interface Sci.* **2000**, *229* (2), 544−549.
(40) Elimelech, M.; Gregory, J.; Jia, X.; Williams, R. A. *Particle Deposition & Aggregation*; Butterworth-Heinemann: Woburn, 1995.
(41) van Loenhout, M. T. J.; Kooij, E. S.; Wormeester, H.; Poelsema, B. Hydrodynamic flow induced anisotropy in colloid adsorption. *Colloids Surf., A* **2009**, *342* (1−3), 46−52.
(42) Mitchell, D. F.; Clark, K. B.; Bardwell, J. A.; Lennard, W. N.; Massoumi, G. R.; Mitchell, I. V. Film Thickness Measurements of SiO_2 by XPS. *Surf. Interface Anal.* **1994**, *21* (1), 44−50.
(43) Bakker, D. P.; Busscher, H. J.; van der Mei, H. C. Bacterial deposition in a parallel plate and a stagnation point flow chamber: microbial adhesion mechanisms depend on the mass transport conditions. *Microbiology* **2002**, *148*, 597−603.
(44) Lüttge, A.; Bolton, E. W.; Lasaga, A. C. An interferometric study of the dissolution kinetics of anorthite: The role of reactive surface area. *Am. J. Sci.* **1999**, *299* (7−9), 652−678.
(45) Fischer, C.; Lüttge, A. Converged surface roughness parameters - A new tool to quantify rock surface morphology and reactivity alteration. *Am. J. Sci.* **2007**, *307* (7), 955−973.
(46) Kline, T. R.; Chen, G. X.; Walker, S. L. Colloidal deposition on remotely controlled charged micropatterned surfaces in a parallel-plate flow chamber. *Langmuir* **2008**, *24* (17), 9381−9385.
(47) Elimelech, M. Effect of Particle-Size on the Kinetics of Particle Deposition under Attractive Double-Layer Interactions. *J. Colloid Interface Sci.* **1994**, *164* (1), 190−199.
(48) Elimelech, M.; Omelia, C. R. Effect of Particle-Size on Collision Efficiency in the Deposition of Brownian Particles with Electrostatic Energy Barriers. *Langmuir* **1990**, *6* (6), 1153−1163.
(49) Huang, X. F.; Bhattacharjee, S.; Hoek, E. M. V. Is Surface Roughness a "Scapegoat" or a Primary Factor When Defining Particle-Substrate Interactions? *Langmuir* **2010**, *26* (4), 2528−2537.
(50) Shen, C. Y.; Huang, Y. F.; Li, B. G.; Jin, Y. Predicting attachment efficiency of colloid deposition under unfavorable attachment conditions. *Water Resour. Res.* **2010**, *46*, W11526, doi:10.1029/2010WR009218.
(51) Burdick, G. M.; Berman, N. S.; Beaudoin, S. P. Describing hydrodynamic particle removal from surfaces using the particle Reynolds number. *J. Nanopart. Res.* **2001**, *3* (5−6), 455−467.
(52) Burdick, G. M.; Berman, N. S.; Beaudoin, S. P. Hydrodynamic particle removal from surfaces. *Thin Solid Films* **2005**, *488* (1−2), 116−123.
(53) Bergendahl, J.; Grasso, D. Prediction of colloid detachment in a model porous media: hydrodynamics. *Chem. Eng. Sci.* **2000**, *55* (9), 1523−1532.
(54) Gregory, J. Interaction of Unequal Double-Layers at Constant Charge. *J. Colloid Interface Sci.* **1975**, *51* (1), 44−51.

(55) Dabros, T. Interparticle Hydrodynamic Interactions in Deposition Processes. *Colloids Surf.* **1989**, *39* (1−3), 127−141.
(56) Adamczyk, Z.; Siwek, B.; Szyk, L. Flow-Induced Surface Blocking Effects in Adsorption of Colloid Particles. *J. Colloid Interface Sci.* **1995**, *174* (1), 130−141.
(57) Ko, C. H.; Bhattacharjee, S.; Elimelech, M. The "shadow effect" in colloid transport and deposition dynamics in granular porous media: Measurements and mechanisms. *Abstr. Pap. Am. Chem. Soc.* **1999**, *217*, U731−U731.
(58) Fischer, C.; Dunkl, I.; von Eynatten, H.; Wijbrans, J. R.; Gaupp, R. Products and timing of diagenetic processes in Upper Rotliegend sandstones from Bebertal (North German Basin, Parchim Formation, Flechtingen High, Germany). *Geological Magazine*, **2012**, Available on CJO doi:10.1017/S0016756811001087.